ISPRS Journal of Photogrammetry and Remote Sensing 87 (2014) 19–27

Contents lists available at ScienceDirect

ISPRS Journal of Photogrammetry and Remote Sensing

journal homepage: www.elsevier.com/locate/isprsjprs

Assessment of the image misregistration effects on object-based change detection

Gang Chen [a,*], Kaiguang Zhao [b], Ryan Powers [c]

[a] Department of Geography and Earth Sciences, University of North Carolina at Charlotte, 9201 University City Blvd, Charlotte, NC 28223, USA
[b] Ohio Agricultural and Research Development Center, School of Environment and Natural Resources, The Ohio State University, Wooster, OH 44691, USA
[c] Integrated Remote Sensing Studio, Department of Forest Resources Management, Faculty of Forestry, University of British Columbia, 2424 Main Mall, Vancouver, BC V6T 1Z4, Canada

ARTICLE INFO

Article history:
Received 3 April 2013
Received in revised form 13 October 2013
Accepted 19 October 2013

Keywords:
Change detection
Object-based
Pixel-based
Misregistration
High-spatial resolution
Accuracy assessment

ABSTRACT

High-spatial resolution remote sensing imagery provides unique opportunities for detailed characterization and monitoring of landscape dynamics. To better handle such data sets, change detection using the object-based paradigm, i.e., object-based change detection (OBCD), have demonstrated improved performances over the classic pixel-based paradigm. However, image registration remains a critical pre-process, with new challenges arising, because objects in OBCD are of various sizes and shapes. In this study, we quantified the effects of misregistration on OBCD using high-spatial resolution SPOT 5 imagery (5 m) for three types of landscapes dominated by urban, suburban and rural features, representing diverse geographic objects. The experiments were conducted in four steps: (i) Images were purposely shifted to simulate the misregistration effect. (ii) Image differencing change detection was employed to generate difference images with all the image-objects projected to a feature space consisting of both spectral and texture variables. (iii) The changes were extracted using the Mahalanobis distance and a change ratio. (iv) The results were compared to the 'real' changes from the image pairs that contained no purposely introduced registration error. A pixel-based change detection method using similar steps was also developed for comparisons. Results indicate that misregistration had a relatively low impact on object size and shape for most areas. When the landscape is comprised of small mean object sizes (e.g., in urban and suburban areas), the mean size of 'change' objects was smaller than the mean of all objects and their size discrepancy became larger with the decrease in object size. Compared to the results using the pixel-based paradigm, OBCD was less sensitive to the misregistration effect, and the sensitivity further decreased with an increase in local mean object size. However, high-spatial resolution images typically have higher spectral variability within neighboring pixels than the relatively low resolution datasets. As a result, accurate image registration remains crucial to change detection even if an object-based approach is used.

1. Introduction

Over the past decades, the global landscape has been continuously reshaped by rapid environmental change (Turner et al., 2007). Therefore, accurate global and regional measures of the landscape state over time are important to improve models and our understanding of the mechanisms causing this change. To date, one of the most widely used technologies for this purpose is remote sensing change detection, which takes advantage of the remote sensing capacities for broad-area synoptic coverage, high temporal frequency and relatively low-cost data acquisition, as well as the advances in digital image processing (Chen et al., 2012).

Multitemporal image registration is an essential pre-process in change detection for ensuring that detected changes are meaningful, and not simply the product of comparing two land-surface objects at different geographic locations (Townshend et al., 1992). Therefore, misregistration errors, if not adequately minimized, can severely compromise the change detection accuracy (Townshend et al., 1992; Dai and Khorram, 1998; Stow, 1999; Roy, 2000; Farin and de With, 2005). Independent studies from Townshend et al. (1992) and Dai and Khorram (1998) demonstrated that a registration accuracy of at least 0.2 pixels is required in order to achieve a change detection with less than 10% error. However, their findings were limited to the use of relatively medium- and low-spatial resolution remote sensing imagery, e.g., 28.5 m Landsat TM and 250/500 m MODIS, and classic pixel-based methods.

* Corresponding author. Tel.: +1 704 687 5947; fax: +1 704 687 5966.
E-mail address: gang.chen@uncc.edu (G. Chen).

0924-2716/$ - see front matter
http://dx.doi.org/10.1016/j.isprsjprs.2013.10.007

Over the last decade, the amount and accessibility of high-spatial resolution (hereafter referred to as h-res) remote sensing images collected from commercial satellites and airborne platforms continued to proliferate globally. While such data sets provide us with unique opportunities for detailed characterization and monitoring of our landscape, the accuracy of change detection algorithms using the classic pixel-based methods is usually reduced by numerous small spurious changes, also called the "salt and pepper" effect (Desclée et al., 2006). To address this issue, the concept of *object-based image analysis* (OBIA) [more recently referred to as *geographic object-based image analysis* (GEOBIA)] was introduced to the change detection domain – *object-based change detection* (OBCD), where image-objects (groups of pixels) are used to model meaningful geographic objects and the task then becomes estimating the changes of image-objects rather than individual pixels (Hall and Hay, 2003; Blaschke, 2010). Improved change detection accuracies were obtained in a range of research fields, such as monitoring forest disturbances, urban development, and natural disasters (Water, 2004; Desclée et al., 2006; Chen and Hutchinson, 2007; Im et al., 2008; Li et al., 2009; Chen et al., 2012). Although OBCD appears promising, image registration remains a critical pre-process, where new challenges are also raised. Specifically, the high spatial and spectral variability of h-res imagery make it sensitive to geometric and radiometric corrections (Baltsavias et al., 2001; Chen and Hay, 2011). As a result, the same level of registration efforts may induce an even higher level of change detection error using h-res imagery. On the other hand, image-objects have proven effective in reducing small spurious changes. An immediate question is: how much these image-objects can compensate for the errors introduced by using the h-res data? It should also be noted that, different from pixels, image-objects are of various sizes and shapes, which may influence change detection accuracy in different ways, although less consideration was given to the quantitative analysis of this effect.

The primary objective of this study was to assess the impacts of misregistration on OBCD using multitemporal h-res imagery. To do so, three types of landscapes dominated by urban, suburban and rural features, were chosen to represent geographic objects of different sizes (small to large) and shapes (simple to complex). Multitemporal images were intentionally misregistered at different errors. Two change detection algorithms based on image-objects and individual pixels were applied to the study areas. Their change detection accuracies were compared and the relationships between object (size and shape) and misregistration were investigated.

2. Methods

2.1. Study areas

Three study areas, located in three counties of North Carolina, USA, were chosen to represent local major land-use/land-cover types, including (i) an urban area (4500 ha) in Mecklenburg County, (ii) a suburban area (4500 ha) in Gaston County, and (iii) an agricultural area (4500 ha) in Lincoln County (Fig. 1). These areas also signified different styles of geographic objects: (i) the urban area (City center of Charlotte and its neighbor) was characterized by high-density anthropogenic features (e.g., large commercial buildings), most of which were compact and had relatively simple roof boundaries as synoptically viewed from the sensor. The changes were mainly caused by converting old buildings/open lands into new multi-story buildings. (ii) The suburban area (south of the City of Gastonia) was dominated by low-density residential communities. High spatial interaction between anthropogenic and natural features was evident by the recent development of urban forests into single-family homes. Consequently, geographic objects, when visualized synoptically, tended to be mixed and the placement of their boundaries was more complex. (iii) The agricultural area was characterized by large farmland, where the size of each land was large and its boundary could be drawn with simple and near-linear lines. The changes were mainly attributed to phenological dynamics of local crops.

2.2. Data and preprocessing

Since all three study areas were within the extent of one SPOT image scene, this research used two dates of SPOT 5 images that were acquired on March 5, 2006 and August 2, 2011. Both images were cloud-free with similar incidence angles of 16.4° and 16.5°, and each one consisted of four 10 m multispectral bands (i.e., green, red, near infrared, and short-wave infrared) and one 5 m panchromatic band.

To retain both the image spectral values and its high-spatial resolution, a Gram–Schmidt algorithm was used to effectively fuse the multispectral channels with the panchromatic band (Laben et al., 2000; Powers et al., 2012). Although a level 2A preprocessing of radiometric and geometric corrections was applied to the individual scenes by the data vendor, minimizing spatial and spectral differences between images taken at different dates was also critical to accurate change detection. In this study, three subsets of the SPOT imagery were extracted to cover the three study areas, with each area covering 4500 ha. Each of these subsets (hereafter *image pairs*) was processed separately using the following steps. The registration was conducted using a second-order affine polynomial and a nearest-neighbor resampling method for RMSEs of 0.28, 0.25 and 0.24 pixels. Although errors still existed, they were comparatively small. In the relative radiometric normalization, linear regression was applied to match the spectral responses of the two-date images based on the digital numbers of unchanged training pixels, located mainly in the regions covered by pavements, buildings and water. This method has proven effective at correcting SPOT 5 time series, with results comparable to those using more rigorous methods, such as the classic 6S model, although fewer parameters are required in the linear regression (El Hajj et al., 2008).

2.3. Simulation of image misregistration

Geometrically, multitemporal images may contain scaling, rotation, translation, and skewing differences (Dai and Khorram, 1998), which are typically caused by one or more factors during data acquisition, such as the differences between sensor's altitudes and attitudes, other than actual landscape changes. In this research, we simplified the misregistration effect by assuming that the errors are equally distributed over the study areas. For each of the three image pairs, the simulation was conducted by intentionally shifting one image against the other at 45° with 30 different errors of $\sqrt{2}i$ pixels ($i = 1, 2, \ldots, 30$) in distance. For example, a pixel at the location of (x, y) was shifted to new locations of $(x + i, y + i)$ after misregistration. This method followed a similar strategy employed by Townshend et al. (1992) and Dai and Khorram (1998). Subpixel misregistration was not performed, as the comparison of two images technically requires their basic sampling units (i.e., pixels) to spatially correspond. Thus, the shifted image will need to be resampled in a subpixel test, and altered pixel spectral values will introduce additional change detection error.

2.4. Change detection

One of the most widely used change detection methods is image differencing, where a predefined threshold is used to separate

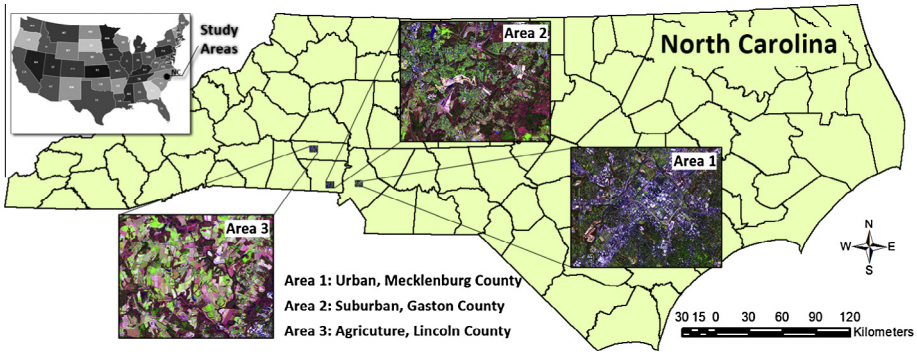

Fig. 1. Three study areas (4500 ha of each) located in three counties of North Carolina, USA, representing urban, suburban and agricultural lands. The SPOT 5 images are color composites using red, near infrared, and short-wave infrared bands. (For interpretation of the references to color in this figure legend, the reader is referred to the web version of this article.)

changed (i.e., higher than a threshold) and non-changed areas (i.e., lower than the threshold) in a difference image. This method was also employed in our research by applying it to all 93 image pairs over three study areas containing and not containing the purposely introduced misregistration errors of $\sqrt{2}i$ pixels ($i = 0,1,2,\ldots,30$). As previously mentioned, the major distinction between pixel-based change detection and OBCD is the basic study units (i.e., pixels versus objects). Image differencing change detection was modified to accommodate this difference, with more details discussed in the following sections.

2.4.1. Object-based method

To perform OBCD, the first step was to generate image-objects using segmentation. A recent review by Chen et al. (2012) divided OBCD algorithms into three types: image-object, class-object and multitemporal-object change detections. For the first two types, multidate images need to be segmented separately. However, it is difficult to produce consistent segmentation results, because images taken at different times tend to contain spectral differences due to variations in Sun angle, sensor look angle and atmospheric transmission. These spectral differences will likely result in discrepancies between image-object geometries (e.g., boundaries), making it challenging to detect true landscape changes (Chen et al., 2012). In this study, we employed a third type of multitemporal-object change detection method, where the two-date images were combined and segmented together in eCognition (Definiens Imaging GmbH, Munich, Germany). Consequently, image-objects from the same geographic locations were spatially corresponding to each other and a direct comparison without considering the object geometry differences was made possible. For all the three study areas, the same set of parameters were used to ensure consistency (i.e., scale parameter: 30, shape: 0.1, and compactness: 0.5).

Image differencing change detection involved the creation of difference images, where an eight-band object-based feature space was created, including (i) four-band spectral responses (DS_G, DS_R, DS_{NIR}, DS_{SWIR}) by subtracting the 2006 segmented images from the 2011 segmented images using the corresponding spectral bands of green (G), red (R), near infrared (NIR), and short-wave infrared (SWIR); and (ii) four-band texture features (DT_G, DT_R, DT_{NIR}, DT_{SWIR}) by calculating standard deviations within individual image-objects and then subtracting the 2006 texture images from the 2011 texture images using G, R, NIR and SWIR bands.

Scatter plots were used to investigate the relationships among the eight bands, where the sample plots representing DS_{SWIR} versus DS_G are displayed in Fig. 2a–c for urban, suburban and agricultural study areas, respectively. The image-objects in the plots were colored using a rainbow gradient to highlight object densities from high (in red) to low (in purple). Obviously, an object far from the mean shows a large multitemporal spectral difference, which should be classified as a change. However, a simple Euclidean distance may not be suitable for defining how far an image-object is from the mean because the density distributions are in ellipsoid shapes indicating a normal distribution of the data in difference images (Fig. 2). As such, we employed the Mahalanobis distance that also took into account the covariance between variables in the feature space. Similar ideas have proven effective at monitoring urban development, forest disturbance and agricultural land conversion (Dai and Khorram, 1998; Ridd and Liu, 1998; Desclée et al., 2006). The Mahalanobis distance was define as

$$\boldsymbol{D} = \sqrt{(\boldsymbol{X}-\boldsymbol{m})^T \boldsymbol{S}^{-1}(\boldsymbol{X}-\boldsymbol{m})} \quad (1)$$

where $\boldsymbol{D}$ is the Mahalanobis distance vector containing all image-objects, $\boldsymbol{X}$ is the two dimensional vector including all image-objects and each object has eight features (DS_G, DS_R, DS_{NIR}, DS_{SWIR}, DT_G, DT_R, DT_{NIR}, DT_{SWIR}); $\boldsymbol{m}$ is the mean vector of these features; and $\boldsymbol{S}$ is the covariance matrix.

To facilitate the analysis of the misregistration effects on change detection, we assumed that 'real' changes are detected from the image pair that contains no purposely introduced registration error, where a change ratio (i.e., percentage of change) was extracted and considered as the ground-truth. Then, this ratio was applied to all the other image pairs with registration errors of $\sqrt{2}i$ pixels ($i = 1,2,\ldots,30$).

2.4.2. Pixel-based method

The pixel-based image differencing change detection was performed in a similar way to the previous OBCD. However, since pixel-based methods work directly on individual pixels, two changes were made: (i) no segmentation was conducted, with all image-objects replaced by pixels during the calculation; and (ii) the four-band texture features (DT_G, DT_R, DT_{NIR}, DT_{SWIR}) were derived by applying a 3-by-3 pixel kernel to extract neighborhood standard deviations for all pixels and then subtracting the 2006 texture images from the 2011 texture images using G, R, NIR and SWIR bands. For comparison purposes, scatter plots representing DS_{SWIR} versus DS_G were created using pixels for urban, suburban and agricultural study areas (Fig. 2d–f), respectively. Similar to the Fig. 2a–c representing image-objects, the pixel-based plots also showed a normal distribution.

2.4.3. Accuracy assessment

The impacts of misregistration on OBCD were assessed and compared among urban, suburban and agricultural lands. Specifically, we first investigated the relationship between

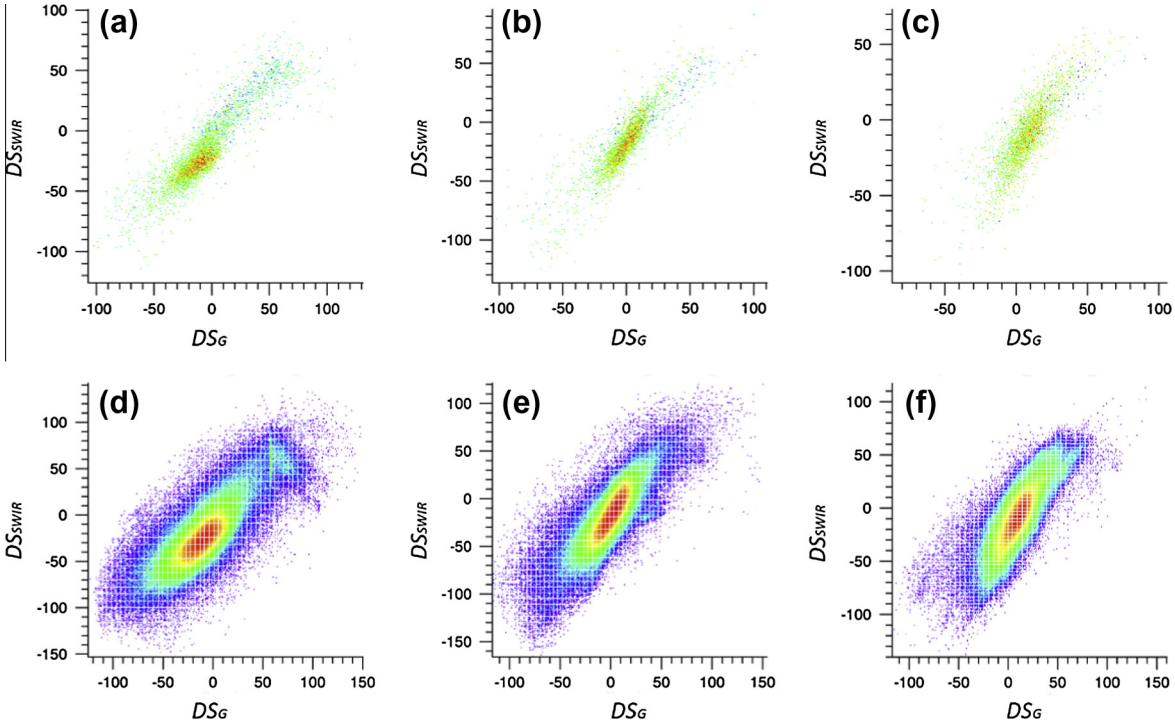

Fig. 2. Scatter plots representing DS_{SWIR} versus DS_G using image-objects (a–c) and pixels (d–f) for the urban (a and d), suburban (b and e) and agricultural (c and f) study areas.

misregistration error and the number and shape of changed objects. The shape was characterized and calculated as a shape index (SI), which measures the complexity of object shape compared to a standard shape (square) of the same size and alleviates the size dependency by using a perimeter (p_i) and area (a_i) for each image-object i (Forman and Godron, 1986):

$$\mathrm{SI} = 0.25p_i/\sqrt{a_i} \tag{2}$$

which equals 1 if the shape is a square. A more complex shape has a higher shape index value. As previously mentioned, we have assumed that the 'real' changes are the detected image-objects or pixels from the image pair that contains no purposely introduced registration error, with the change locations stored in an array C_{real}. The locations of the detected changes from a misregistered image pair were defined as C_{misreg}. Therefore, the true changes were presented in the overlapped areas C_{true} ($C_{real} \cap C_{misreg}$). Consequently, the change detection error percentage (Err) can be defined as

$$\mathrm{Err} = \left(1 - \frac{\text{Area of } C_{true}}{\text{Area of } C_{misreg}}\right) \times 100\% \tag{3}$$

On the basis that change ratio remains the same, if C_{real} and C_{misreg} are perfectly overlapped, C_{true} is equal to C_{misreg}, resulting in a change detection error of zero. If there is no overlap, the error is 100% as C_{true} contains no pixels/image-objects. In this research, three change ratio values were used to specify the actual changes in the three study areas respectively. To determine the ratio absolute values, 50 points were randomly extracted from each study area, with each point corresponding to a ground area (i.e., 25 m^2) covered by one SPOT image pixel. One-meter NAIP (National Agriculture Imagery Program) aerial photographs collected in 2006 and 2011 were used as ground truth data to help determine whether actual changes occurred at these points. A 'change point' was defined as a ground point in which more than 50% of the 25 m^2 area has changed. The change ratio was then calculated via a simple operation – a ratio between the number of change points and the total number of points (i.e., 50). By following this method, three change ratio values of 8%, 8% and 10% were derived for the urban, suburban and agriculture study areas respectively. The same ratio values were used in both the pixel-based and object-based approaches to calculate C_{true} and C_{misreg} (Eq. (3)) because the ratio values were directly derived from NAIP image interpretation and should remain constant no matter which image pairs (with different registration errors) are used. Although a slight change in the ratio absolute value may have a considerable impact on the areas detected as change, our experiments indicated that changing the ratio absolute value had little impact on the calculation of change detection error percentage (Err) when misregistration was smaller than two pixels. We note that misregistration in most remote sensing projects is typically within this error range.

3. Results and discussion

3.1. Impacts of misregistration on object size and shape

Fig. 3 shows three image subsets of the same spatial scale representing (a1) urban, (b1) suburban and (c1) agricultural areas, and a2, b2 and c2 are sample segmentation results from the image pairs that contain no intentionally introduced registration error. As expected, the *mean object size* (MOS) for the agricultural area was the largest of the three (i.e., 1.25 ha), as large croplands tend to be internally homogenous due to similar planting and cropping patterns. Individual buildings and other facilities extracted from the urban center have the smallest MOS (i.e., 0.75 ha), while the MOS of suburban residential area is in the between (i.e., 1.10 ha). Theoretically, the anthropegenic features from the urban center are typically larger than the individual homes in the suburban residential area. However, the low-density suburban also contains relatively large forest stands, parks and barren lands (e.g., an underdevelopment area with bright tones close to the right side of Fig. 3b1). We also recognize that blending with the surrounding vegetation made it challenging to extract individual homes from 5 m spatial resolution imagery (Fig. 3b2).

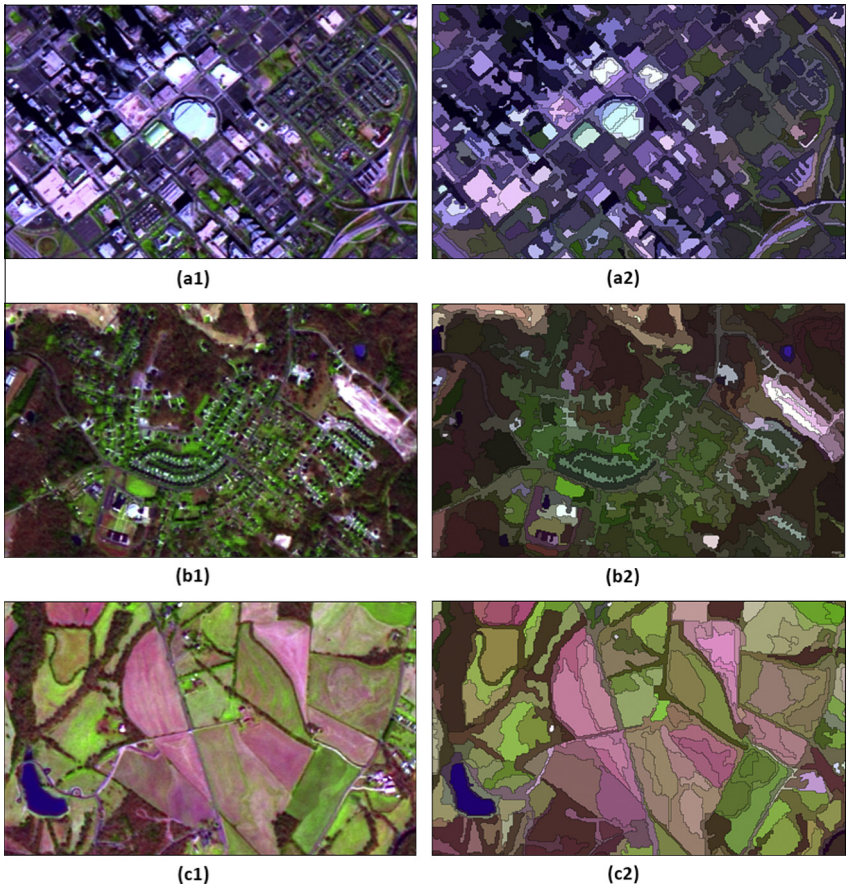

Fig. 3. Three image subsets of the same spatial scale representing (a1) urban, (b1) suburban and (c1) agricutural areas, and a1, b2 and c2 are sample segmentation results from the image pairs that contain no purposely introduced registration error.

When a misregistration error was introduced, higher spectral variability was also introduced to the multitemporal images. Even if a geographic object remained the same over time, misregistration caused a shift in the boundary. Consequently, more boundary regions were generated. With the same set of segmentation parameters (i.e., scale, shape and compactness), more and smaller image-objects were expected. However, the findings from the three study areas showed slightly different trends. Specifically, Fig. 4 illustrates the relationships between misregistration error and the size of two types of image-objects: all objects (light colors) and only the changes (dark colors), for urban (red[1]), suburban (blue) and agricultural (purple) lands. When considering the size change for all image-objects (light colors), the three areas exhibit similar trends, which can be divided into three phases: (i) slight increase when the misregistration error is relatively small (e.g., lower than 3 pixels), (ii) decrease when the misregistration error increases (e.g., between 3 pixels and 10 pixels), and (iii) no change when the misregistration error is large (e.g., larger than 10 pixels). This could be explained in three steps: (i) since an object boundary in h-res imagery often spans one or more pixels, the slight shift between the multidate images probably has increased the boundary width. Small objects or the objects with a linear shape (e.g., roads) merged into the neighboring image-objects. (ii) With the increase in misregistration error, small objects were detected and meanwhile, large objects were divided into smaller pieces by the fake 'new boundaries'. (iii) No noticeable change occurred when the misregistration error was too large, as the high spectral variability spread over the entire area. We further

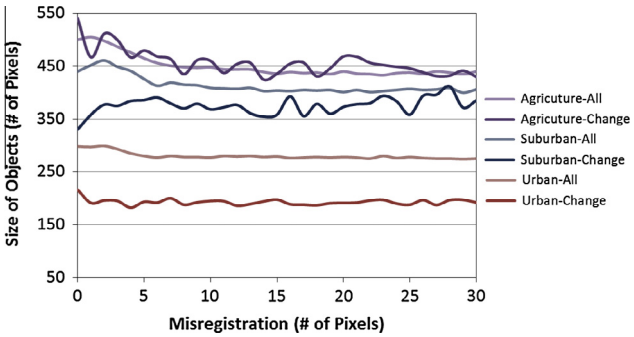

Fig. 4. The relationships between misregistration error and the size of (i) all image-objects and (ii) only the changes for urban, suburban and agricultural areas.

noticed that the trend line for the urban area (light red in Fig. 4) is relatively flat compared to the trends of suburban and agricultural areas. This may be explained by the fact that urban areas contain more compact objects (Fig. 3a2), where the shift in boundaries during the first two misregistration phases has a reduced impact.

Fig. 4 also shows the relationships between misregistration error and the size of image-objects detected as the change using the aforementioned OBCD method (Section 2.4.1) for urban (light red), suburban (light blue) and agricultural (light purple) lands. Overall, the trend lines representing the change (light colors in Fig. 4) are similar to those derived from all image-objects (dark colors in Fig. 4). However, the differences still remain: (i) the 'change' lines fluctuate at a higher rate, which is correlated with the MOS.

[1] For interpretation of color in Fig. 4, the reader is referred to the web version of this article.

This makes sense, as a specific change ratio (i.e., percentage) was used to extract changes in this research. If the MOS is large (e.g., 1.25 ha in the agricultural area), the object sizes tend to have a greater dynamic range. The addition or removal of image-objects would highly affect the average object size. On the other hand, relatively small MOS tend to produce similarly sized image objects and, subsequently, a smooth trend line (e.g., dark red in Fig. 4 representing the urban area with MOS of 0.75 ha). An extreme case is where individual image-objects contain only a single pixel (i.e., pixel-based change detection), the average object size would remain the same, regardless of the introduced misregistration errors. (ii) We also determined that in the urban area, the size of 'change' image-objects is always below the average size of all image-objects (light red versus dark red in Fig. 4). With the increase in MOS, the two trend lines are getting closer (light blue versus dark blue in Fig. 4). For large agricultural lands, the two lines are interacting with each other (light purple versus dark purple in Fig. 4). This trend could be explained by the reality that the urban area contained a higher spectral variability – which accounts for why smaller image-objects were generated – that resulted in the misregistration induced change showing a greater 'salt-and-pepper' effect. However, this 'salt-and-pepper' effect was more sever using the pixel-based approach.

Similar to what was observed with object size, the object shape was also affected by misregistration. Fig. 5 represents the relationships between misregistration error and the shape index of image-objects detected as the change for urban, suburban and agricultural areas. When the multidate images contain no registration error (i.e., misregistration equals 0), the detected urban image-objects are more similar to squares with the lowest index value of 1.22, while the index values for suburban and agricultural image-objects are higher, i.e., 1.25 and 1.37, respectively. The agricultural lands have the largest average shape index value, because most of the image-objects have a strip shape resulting in a larger perimeter for a certain object size (Fig. 3c2). With the increase in misregistration error, the shape index values slightly increase for the urban and agricultural areas and plateaus when the error is 3 pixels. Then, the values decrease until the misregistration error reaches 10 pixels, after which the lines become stable. This is similar to the trends described in Fig. 4. However, one exception is the shape change in the suburban area. In particular, when the misregistration increases from 0 to 5 pixels, the object shape has a dramatic change from 1.25 to 1.41 (13% increase), a value that approaches that of the agricultural lands. The main reason is that many of the suburban image-objects contained rugged boundaries with elogated shapes, such as underdevelopment areas and new communities where major changes typically occurred (bright tones in Fig. 3b2). In contrast, their neighbors were typically forest stands bounded by roads that had relatively simple boundaries. The misregistration created more complex boundaries than the simple ones, which unavoidably increased the shape index value.

3.2. Impacts of misregistration on change detection error

The change detection errors were calculated for both the object-based and the pixel-based methods, with their results presented in Fig. 6 for (a) urban, (b) suburban and (c) agricultural areas. Similarly trends can be found for all the three areas (i.e., change detection error increases with the increase in misregistration error). When a small shift between the two-date images occurs (e.g., smaller than 10 pixels), the change detection error increases. For example, even if the misregistration is only a single pixel, the change detection error increases by 22.7% (pixel-based) and 21.26% (object-based) for urban, 22.0% (pixel-based) and 21.6% (object-based) for suburban, and 19.0% (pixel-based) and 18.4% (object-based) for agricultural areas (Fig. 6). When the shift between the images is larger than 10 pixels, the errors gradually increase up to approximately 60%. Although the change detections using pixels and objects have similar error trends, the object-based method performs relatively better by reducing the average errors by 0.7%, 1.3% and 4.5% for urban, suburban and agricultural areas, respectively. Clearly, the larger MOS in the area, the better the object-based paradigm performs.

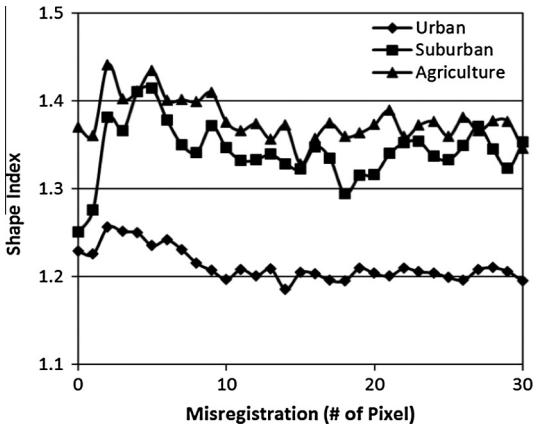

Fig. 5. The relationships between misregistration error and the shape index of image-objects detected as changes for urban, suburban and agricultural areas.

To quantify the relationships between change detection error and misregisration error, all six trend lines in Fig. 6 were simulated using logarithmetric equations, with R^2 ranging from 0.88 to 0.98 (Table 1). In order to reduce the misregistration-caused change detection error to 10%, the shifts between the multidate images are required to be less than 0.03 pixels (pixel-based) and 0.07 pixels (object-based) for urban, 0.05 pixels (pixel-based) and 0.07 pixels (object-based) for suburban, and 0.10 pixels (pixel-based) and 0.23 pixels (object-based) for agricultural areas (Table 1). As anticipated, both methods show that large landscape features (e.g., agricultural lands) are not as sensitive as small features (e.g., built-up areas) to the misregistration. Compared to the results using individual pixels, the object-based method consistently performs better by 133%, 40% and 130% for urban, suburban and agricultural areas. However, it should be noted that the two types of methods reacted differently for different levels of changes. In theory, the changes extracted from multidate images are due to the large spectral difference between pixels/image-objects from the same geographic locations. After misregistration is introduced, whether 'new' changes will be detected actually relies on the disagreement between the pixels/image-objects with their neighbors.

Figs. 7 and 8 show two examples of high and low spectral differences between the changed areas and their neighbors. Specifically, Fig. 7 represents the change from the underdevelopment to the new residential. Since the barren land in the underdevelopment area has very high spectral reflectance compared to the other areas (e.g., trees in either leaf-off (2006 image in Fig. 7) or leaf-on (2011 image in Fig. 7) condition), misregistration at small errors (from 1 to 3 pixels) has a relatively low impact on change detection, although the results generated by the pixel-based method tend to have a more pronounced pepper-and-salt effect. Fig. 8 illustrates the changes in an agricultural area that are due to crop phenological variability. Contrary to the case in Fig. 7, when small misregistration errors occur, a big portion of the 'real' change disappears (Fig. 8a0 versus Fig. 8a1–a3) using OBCD; while, the pixel-based method is better able to retain changes (Fig. 8b0 versus Fig. 8b1–b3). One potential reason is that large agricultural lands generated large-sized image-objects, and their spectral responses were similar to those of their neighboring lands. Upon misregistration,

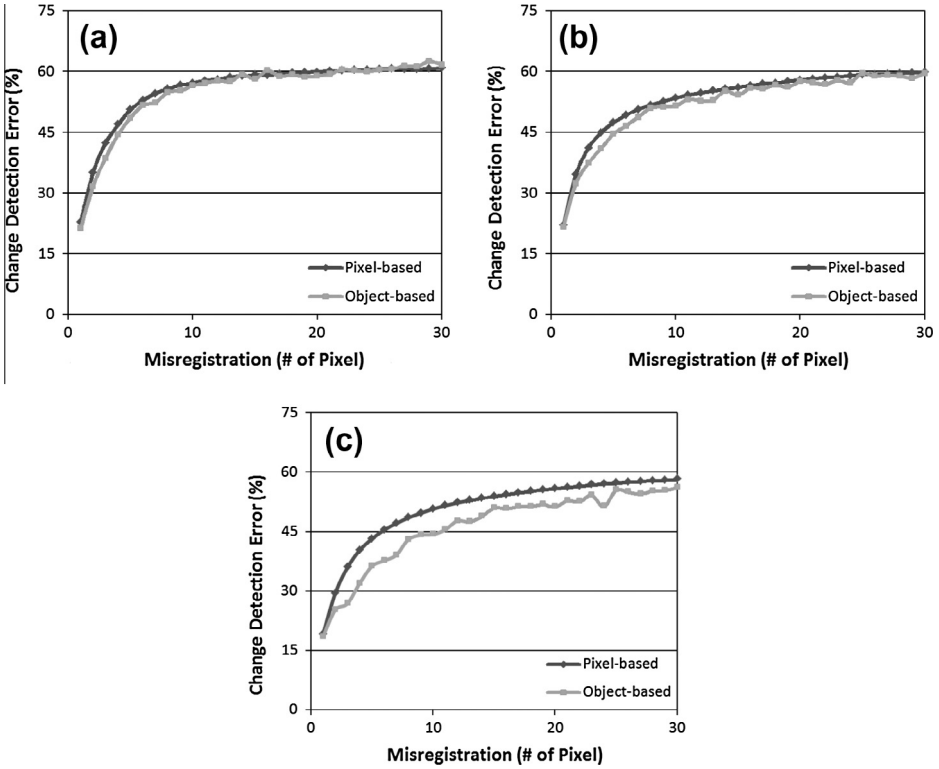

Fig. 6. The relationships between misregistration error and change detection error (pixel-based versus object-based) for (a) urban, (b) suburban and (c) agricultural areas.

Table 1
Simulation of change detection error (y) as a function of misregistration error (x).

Study area	Method	Equation	R^2	x (pixel), when $y = 0.1$[a]
Urban	Pixel-based	$y = 9.50 \ln(x) + 32.04$	0.88	0.03
	Object-based	$y = 10.65 \ln(x) + 28.47$	0.91	0.07
Suburban	Pixel-based	$y = 9.583 \ln(x) + 29.53$	0.94	0.05
	Object-based	$y = 10.21 \ln(x) + 26.59$	0.96	0.07
Agriculture	Pixel-based	$y = 10.61 \ln(x) + 24.27$	0.96	0.10
	Object-based	$y = 11.61 \ln(x) + 17.29$	0.98	0.23

[a] $y = 0.1$ indicates a 10% change detection error.

changes in other areas may become more evident, which falsely removed the changes in the current area represented by large-size image-objects (Fig. 8a1–a3). This leads to a potential issue of using the object-based paradigm in change detection, where large-area non-substantial changes may not be detected using OBCD even when a small registration error occurs. We note that the application of an inaccurate change ratio may have also caused this issue.

Previous research conducted by Townshend et al. (1992) and Dai and Khorram (1998) have quantified the effects of misregistration on change detection using pixel-based approaches and lower spatial resolution images (i.e., 250/500 m MODIS and 28.5 m Landsat TM). Both studies suggest a registration accuracy of at least 0.2 pixels for achieving a change detection error of 10%. The comparison between their results and ours indicates that different registration standards may be applied to images of different spatial resolutions. For the h-res data, the spectral variability within the neighboring pixels is much higher, making accurate image registration increasingly important for minimizing

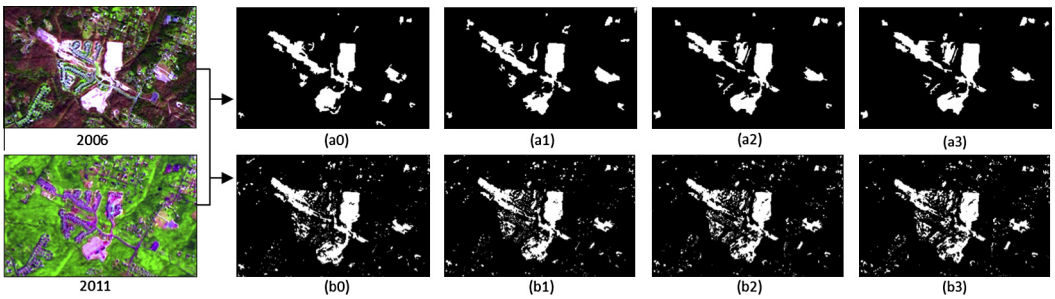

Fig. 7. The 2006 and 2011 images and the detected changes in white (i.e., from the underdevelopment to the new residential), using object-based (ai) and pixel-based (bi) methods where the misregistration error is i ranging from 0 to 3 pixels.

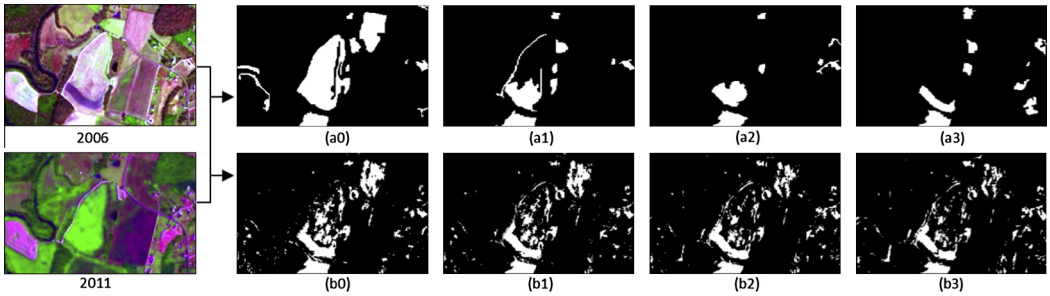

Fig. 8. The 2006 and 2011 images and the detected changes in white (i.e., crop phenological variability), using object-based (a*i*) and pixel-based (b*i*) methods where the misregistration error is *i* ranging from 0 to 3 pixels.

change detection errors, particularly for the areas containing fine-scale features (e.g., urban regions). It is also worth noting that even using the object-based method, it is still difficult to fully compensate for the negative impacts of misregistration on change detection when the image spatial resolution is increased. In addition, unlike the pixel-based approaches using individual pixels, OBCD requires a unique segmentation procedure to extract image-objects (i.e., internally coherent segments) as the basic study units. However, geo-objects (i.e., geographic objects in the real world) are scale dependent. Even for the same landscape features, these objects could be extracted at a course scale (e.g., forest stands), while they could also be extracted at a fine scale (e.g., small tree clusters). The inconsistency between image-objects and geo-objects lead to over-segmentation or under-segmentation (Castilla and Hay, 2008). Hence, under a misregistration condition, the concept of multitemporal objects remains complicated. The potential errors likely to be introduced during both the segmentation and the threshold-based change detection processes add a level of complexity greater than that when applying pixel-based approaches.

4. Conclusions

Recent research efforts have indicated the improved performance of detecting spatially detailed changes in h-res imagery by shifting from the classic pixel-based paradigm to the object-based paradigm (i.e., OBCD); however, less consideration was given to the misregistration issue in OBCD. In this research, we examined the impacts of misregistration on OBCD using h-res multidate SPOT 5 imagery (5 m) for three types of landscapes dominated by urban, suburban and rural features. With the increase in misregistration error, we found that, both the size and shape of the detected 'change' objects showed dynamics, though in relatively small ranges, indicating that misregistration has a comparatively low impact on object size and shape. An exception occurred in the suburban area, where residential or underdevelopment image-objects contained rugged boundaries with elongated shapes, while their neighbors were typically forest stands bounded by roads that had relatively simple boundaries. Small misregistration errors (e.g., lower than 5 pixels) may result in the generation of more image-objects with complex boundaries (i.e., higher shape index values). We further note that, for the agricultural area with large MOS, the detected 'change' objects possessed a mean size similar to that of all objects. As MOS became smaller (e.g., suburban or urban), the size of 'change' objects was getting much smaller than that of all objects in the area. The impacts of misregistration on change detection accuracy were evaluated by comparing OBCD with a pixel-based approach. For all the three areas, OBCD proved less sensitive to misregistration. Additionally, the larger MOS in the study area, the better the OBCD performed. However, it is important to understand that for the h-res data, the spectral variability within the neighboring pixels is much higher than that in relatively low resolution data, making accurate image registration more crucial to change detection. To achieve a change detection error of 10%, the best result from OBCD was 0.23 pixels for the large and homogeneous agricultural area. While this result is typical for multiple landscape features if using medium/low resolution images and pixel-based approaches (Townshend et al., 1992; Dai and Khorram, 1998), our findings suggest that change detection using the object-based paradigm is unlikely to fully compensate for the negative impacts of misregistration on change detection due to an increase in image spatial resolution. But, we note that the conclusion made in this study was based on the use of a multitemporal change detection approach. If other change detection approaches are used, e.g., class-object change detection (Chen et al., 2012), misregistration may have a lower impact on high-spatial resolution imagery. However, additional processes and/or rules are possibly required (e.g., object-based classification), which could introduce extra errors.

Acknowledgments

This research was supported by the University of North Carolina at Charlotte Faculty Research Grant and the College of Liberal Arts and Sciences Seed Grant. The authors acknowledge the valuable discussions with Dr. Thomas Blaschke at the University of Salzburg and the insightful comments from the Editor and two anonymous reviewers.

References

Baltsavias, E., Pateraki, M., Zhang, L., 2001. Radiometric and geometric evaluation of Ikonos GEO images and their use for 3D building modelling. In: Proc. Joint ISPRS Workshop High Resolution Mapping from Space 2001. Hannover, 19–21 September. Institute of Photogrammetry & Geoinformation, University of Hannover, 21 pp. (on CD ROM).

Blaschke, T., 2010. Object based image analysis for remote sensing. ISPRS Journal of Photogrammetry and Remote Sensing 65 (1), 2–16.

Castilla, G., Hay, G.J., 2008. Image-objects and geo-objects. In: Blaschke, T., Lang, S., Hay, G.J. (Eds.), Object-Based Image Analysis Spatial Concepts for Knowledge-driven Remote Sensing Applications. Springer-Verlag, pp. 91–110 (Chapter 1.5).

Chen, G., Hay, G.J., 2011. A support vector regression approach to estimate forest biophysical parameters at the object level using airborne Lidar Transects and QuickBird Data. Photogrammetric Engineering and Remote Sensing 77 (7), 733–741.

Chen, Z., Hutchinson, T.C., 2007. Urban damage estimation using statistical processing of satellite images. Journal of Computing in Civil Engineering 21 (3), 187–199.

Chen, G., Hay, G.J., Carvalho, L.M.T., Wulder, M.A., 2012. Object-based change detection. International Journal of Remote Sensing 33 (14), 37–41.

Dai, X., Khorram, S., 1998. The effects of image misregistration on the accuracy of remotely sensed change detection. IEEE Transactions on Geoscience and Remote Sensing 36 (5), 1566–1577.

Desclée, B., Bogaert, P., Defourny, P., 2006. Forest change detection by statistical object-based method. Remote Sensing of Environment 102 (1–2), 1–11.

El Hajj, M., Begue, A., Lafrance, B., Hagolle, O., Dedieu, G., Rumeau, M., 2008. Relative radiometric normalization and atmospheric correction of a spot 5 time series. Sensors 8, 2774–2791.

Farin, D., de With, P.H.N., 2005. Misregistration errors in change detection algorithms and how to avoid them. IEEE International Conference on Image Processing 2, 438–441.

Forman, R.T.T., Godron, M., 1986. Landscape Ecology. John Wiley & Sons, New York, 619 pp.

Hall, O., Hay, G.J., 2003. Amultiscale object-specific approach to digital change detection. International Journal of Applied Earth Observation and Geoinformation 4 (4), 311–327.

Im, J., Jensen, J.R., Tullis, J.A., 2008. Object-based change detection using correlation image analysis and image segmentation. International Journal of Remote Sensing 29 (2), 399–423.

Laben, C.A., Bernard, V., Brower, W., 2000. Process for enhancing the spatial resolution of multispectral imagery using pan-sharpening. US Patent 6.011.875.

Li, X., Yeh, A.G., Qian, J., Ai, B., Qi, Z., 2009. A matching algorithm for detecting land use changes using case-based reasoning. Photogrammetric Engineering & Remote Sensing 75 (11), 1319–1332.

Powers, R.P., Hay, G.J., Chen, G., 2012. How wetland type and area differ through scale: a GEOBIA case study in Alberta's Boreal Plains. Remote Sensing of Environment 117, 135–145.

Ridd, M.K., Liu, J.J., 1998. A comparison of four algorithms for change detection in an urban environment. Remote Sensing of Environment 63 (2), 95–100.

Roy, D.P., 2000. The impact of misregistration upon composited wide field of view satellite data and implications for change detection. IEEE Transactions on Geoscience and Remote Sensing 38 (4), 2017–2032.

Stow, D.A., 1999. Reducing the effects of misregistration on pixel-level change detection. International Journal of Remote Sensing 20 (12), 2477–2483.

Townshend, J.R.G., Justice, C.O., Gurney, C., McManus, J., 1992. The impact of misregistration on change detection. IEEE Transactions on Geoscience and Remote Sensing 30 (5), 1054–1060.

Turner, B.L., Lambin, E.F., Reenberg, A., 2007. The emergence of land change science for global environmental change and sustainability. Proceedings of the National Academy of Sciences 104, 20666–20671.

Water, W., 2004. Object-based classification of remote sensing data for change detection. ISPRS Journal of Photogrammetry & Remote Sensing 58 (3–4), 225–238.